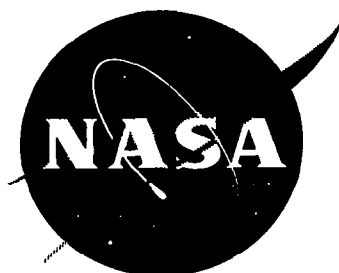


NASA
CR
121143
c.1



LOAN COPY: RETURN
AFWL (5 UL)
KIRTLAND AFB, N.

NASA-CR-121143

Gulf-GA-A12506

0062695

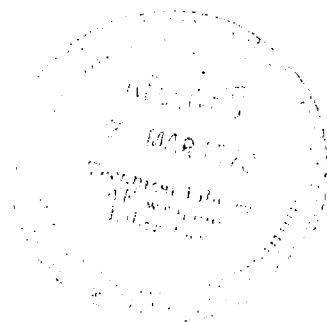


TECH LIBRARY KAFB, NM

DEVELOPMENT OF CHEMICALLY VAPOR DEPOSITED
RHENIUM EMITTERS OF (0001) PREFERRED
CRYSTAL ORIENTATION

Contract No. NAS 3-15323

Prepared for
National Aeronautics and Space Administration
Lewis Research Center
Cleveland, Ohio 44135



Report written by:
L. Yang
R. G. Hudson

Issued: February 19, 1973

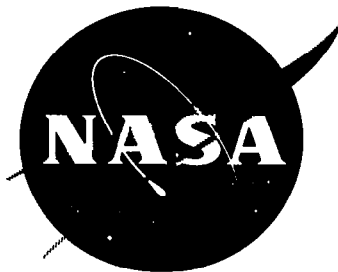
GENERAL ATOMIC COMPANY, P. O. BOX 81608, SAN DIEGO, CALIFORNIA 92138



0062695

GULF GENERAL ATOMIC

~~P. O. BOX 81608, SAN DIEGO, CALIFORNIA 92138~~



✓ NASA-CR-121143

✓ Gulf-GA-A12506

call #

✓
DEVELOPMENT OF CHEMICALLY VAPOR DEPOSITED
RHENIUM EMITTERS OF (0001) PREFERRED
CRYSTAL ORIENTATION

Sponsored by
National Aeronautics and Space Administration
Lewis Research Center

*✓ Young, L.
Hudson, R. G.*

Technical Management
NASA-Lewis Research Center
Nuclear Systems Division
J. J. Ward

Project 6136
Contract NAS 3-13463

✓
Issued: February 19, 1973

NOTICE

This report was prepared as an account of Government sponsored work. Neither the United States, nor the National Aeronautics and Space Administration (NASA), nor any person acting on behalf of NASA:

- A. Makes any warranty or representation, expressed or implied, with respect to the accuracy, completeness, or usefulness of the information contained in this report, or that the use of any information, apparatus, method, or process disclosed in this report may not infringe privately owned rights; or
- B. Assumes any liabilities with respect to the use of , or for damages resulting from the use of any information, apparatus, method or process disclosed in this report.

As used above, "person acting on behalf of NASA" includes any employee or contractor of NASA, or employee of such contractor, to the extent that such employee or contractor of NASA, or employee of such contractor prepares, disseminates, or provides access to, any information pursuant to his employment or contract with NASA, or his employment with such contractor.

Requests for copies of this report should be referred to:

National Aeronautics and Space Administration
Office of Scientific and Technical Information
Attention: AFSS-A
Washington, D. C. 20546

PREVIOUS REPORTS

Contract NAS 5-1253	GA-3523, Final Report for the Period Ending August 31, 1962.
Contract NAS 3-2301	GA-3642, Final Report for the Period Ending August 31, 1962.
Contract NAS 3-2532	GA-4769, Final Report for the Period Ending August 31, 1963. Part I and Part II.
Contract NAS 3-4165	NASA CR-54322, GA-5665, Summary Report for the Period September 1, 1963 through August 31, 1964.
Contract NAS 3-6471	NASA CR-54980, GA-6860, Summary Report for the Period September 1, 1964 through November 23, 1965.
Contract NAS 3-8504	NASA CR-72315, GA-7682, Summary Report for the Period November 23, 1965 through January 31, 1966.
Contract NAS 3-8504	NASA CR-72327, GA-7745, Semi-Annual Report for the Period February 1, 1967 through July 31, 1967.
Contract NAS 3-6471	NASA CR-72517, GA-8974, Summary Report for the Period November 23, 1965 through September 30, 1966.
Contract NAS 3-8504	NASA CR-72627, GA-8956, Summary Report for the Period February 1, 1967 through July 31, 1969.
Contract NAS 3-8504	NASA CR-72947, Gulf-GA-11035, Summary Report for the Period August 1, 1969 through December 7, 1970.
Contract NAS 3-11822	NASA CR-120839, Gulf-GA-A11049, Summary Report for the Period June 1, 1968 through January 31, 1969.
Contract NAS 3-13471	NASA CR-120945, Gulf-GA-A12121, Fabrication and Testing of (U, Zr) C-Fueled/Tungsten-Clad Specimens for Irradiation in the Plum Brook Reactor Facility, Issued July 12, 1972.
Contract NAS 3-15323	NASA-CR-120995, Gulf-GA-A12237, Examination of UC-ZrC After Long Term Irradiation at Thermion Temperature, Issued December 21, 1972.

CONTENTS

SUMMARY	1
1. INTRODUCTION.....	2
2. SAMPLE PREPARATION	3
2.1. Deposition Apparatus	3
2.2. Chlorination Studies	3
2.3. Deposition Procedures	7
3. SAMPLE EVALUATION	9
4. EVALUATION RESULTS	10
4.1. Screening Study	10
4.2. Optimization Study	15
4.3. Reproducibility Studies	22
5. PREPARATION OF CYLINDRICAL RHENIUM EMITTERS	26
APPENDIX A: INTERDIFFUSION BETWEEN RHENIUM AND TANTALUM AT 1500°C	31
APPENDIX B: PREPARATION OF TWELVE CHLORIDE- FLUORIDE DUPLEX TUNGSTEN EMITTERS	34
REFERENCES.....	40

FIGURES

1.	Rhenium deposition apparatus.....	4
2.	Configuration and dimensions of molybdenum mandrel.....	6
3.	Microstructures of CVD rhenium samples for screening study. The numbers shown in parentheses beside each sample designation are chlorine flow rate in standard c. c. /min., rhenium pellet temperature in °C, and mandrel temperature in °C.	13-14
4.	Distribution of the <0001> axes in ten rhenium screening study samples	16
5.	Microstructures of some CVD rhenium samples for optimization study. The numbers shown in parentheses beside each sample designation are chlorine flow rate in standard c. c. /min., rhenium pellet temperature in °C, and mandrel temperature in °C	18
6.	Distributions of the < 0001> axes in ten rhenium optimization study samples	21
7.	Distribution of the < 0001> axes in five rhenium reproducibility study samples	24
8.	Distribution of the <0001> axes in as-deposited cylindrical rhenium emitter No. 1	28
9.	Distribution of the <0001> axes in cylindrical rhenium emitter No. 2	29
10.	Distribution of the <0001> axes in cylindrical rhenium emitter No. 3	30
11.	Ta-Re interface after 100 hours at 1500°C	32
12.	Ta-Re interface after 1000 hours at 1500°C	33
13.	Typical microstructures of the fluoride tungsten substrate after outgassing in vacuum at 1800°C for 12 hours.....	35
14.	Distributions of the <110> axes in cylindrical duplex tungsten emitters, numbers 1 through 12	38

TABLES

1.	Impurity Contents of Rhenium Powder Procured from Cleveland Refractory Metals.	5
2.	Cl/Re Atom Ratio of the Chlorination Product Formed under Various Chlorination Conditions.	8
3.	Deposition Conditions and Results of Screening Deposition Tests	11
4.	Impurity Contents in Rhenium Samples for Screening Study	12
5.	Deposition Conditions and Results of Optimization Deposition Tests	17
6.	Impurity Contents in Rhenium Samples for Optimization Study	20
7.	Vacuum Emission Results for Seven Optimization Study Samples	23
8.	Vacuum Emission Results for Five Reproducibility Study Samples	25
9.	Impurity Contents of Fluoride Tungsten Substrates	36

This page intentionally left blank

SUMMARY

Rhenium thermionic emitters were prepared by the pyrolysis of rhenium chlorides formed by the chlorination of rhenium pellets. The impurity contents, microstructures, degrees of (0001) preferred crystal orientation, and vacuum electron work functions of these emitters were determined as a function of deposition parameters, such as substrate temperature, rhenium pellet temperature and chlorine flow rate. A correlation between vacuum electron work function and degree of (0001) preferred crystal orientation was established. Conditions for depositing porosity-free rhenium emitters of high vacuum electron work functions were defined. Finally, three cylindrical rhenium emitters were prepared under the optimum deposition conditions.

DEVELOPMENT OF CHEMICALLY VAPOR DEPOSITED RHENIUM EMITTERS OF (0001) PREFERRED CRYSTAL ORIENTATION

1. INTRODUCTION

In the direct conversion of heat into electrical energy by thermionic means, the output of the converter is strongly affected by the vacuum work function of the electron emitter. High vacuum work function of the emitter raises converter output and improves conversion efficiency. The (0001) lattice plane of a rhenium single crystal has been shown to possess a very high vacuum work function of 5.59 eV,⁽¹⁾ and a cesiated converter containing such a rhenium emitter exhibited outstanding thermionic performance.⁽²⁾ Single crystal emitters, though of fundamental interest, are impractical from the point of view of cost and configuration required in engineering devices. A CVD polycrystalline rhenium emitter exhibiting (0001) preferred crystal orientation was prepared by the pyrolysis of rhenium chloride⁽³⁾ and yielded a vacuum work function of 5.1 eV.⁽⁴⁾ Although the feasibility of preparing a high work function rhenium emitter has been demonstrated, no effort has been made to correlate the deposition parameters with the properties of the deposit obtained. It is hoped that through a thorough understanding of the effect of the deposition parameters on the physical and metallurgical characteristics of the deposit, high work function rhenium emitters can be reproducibly prepared for use in thermionic devices.

2. SAMPLE PREPARATION

2.1. DEPOSITION APPARATUS

Figure 1 shows schematically the deposition apparatus. The rhenium chloride used for the preparation of the rhenium deposit was formed inside the deposition apparatus in a 1 inch diameter quartz reservoir by chlorination of rhenium pellets with high purity chlorine. These rhenium pellets (1/4 inch diameter, 1/16 inch thickness, 80% theoretical density) were prepared by cold pressing 200 mesh rhenium powder at 10,000 psi and sintering the pressed pellets in vacuum at 1400°C for 15 hours. The impurity contents of the rhenium powder used are shown in Table 1. The molybdenum mandrel (1 inch diameter, 1/4 inch thickness, see Fig. 2) onto which the rhenium was deposited was supported on a ceramic tube and heated by high frequency induction. During the deposition, the mandrel was rotated at 2 rpm through a rubber O-ring seal and its temperature was followed by sighting an optical pyrometer into a hohlraum drilled into the backside of the mandrel. The mandrel was surrounded by a 2 inch diameter quartz jacket which was pumped continuously during the deposition to remove the reaction product. The other components shown in Fig. 1 are self-explanatory.

2.2. CHLORINATION STUDIES

Twenty-one runs were carried out to determine the Cl/Re atom ratio in the chlorination product as a function of chlorine flow rate, rhenium pellet

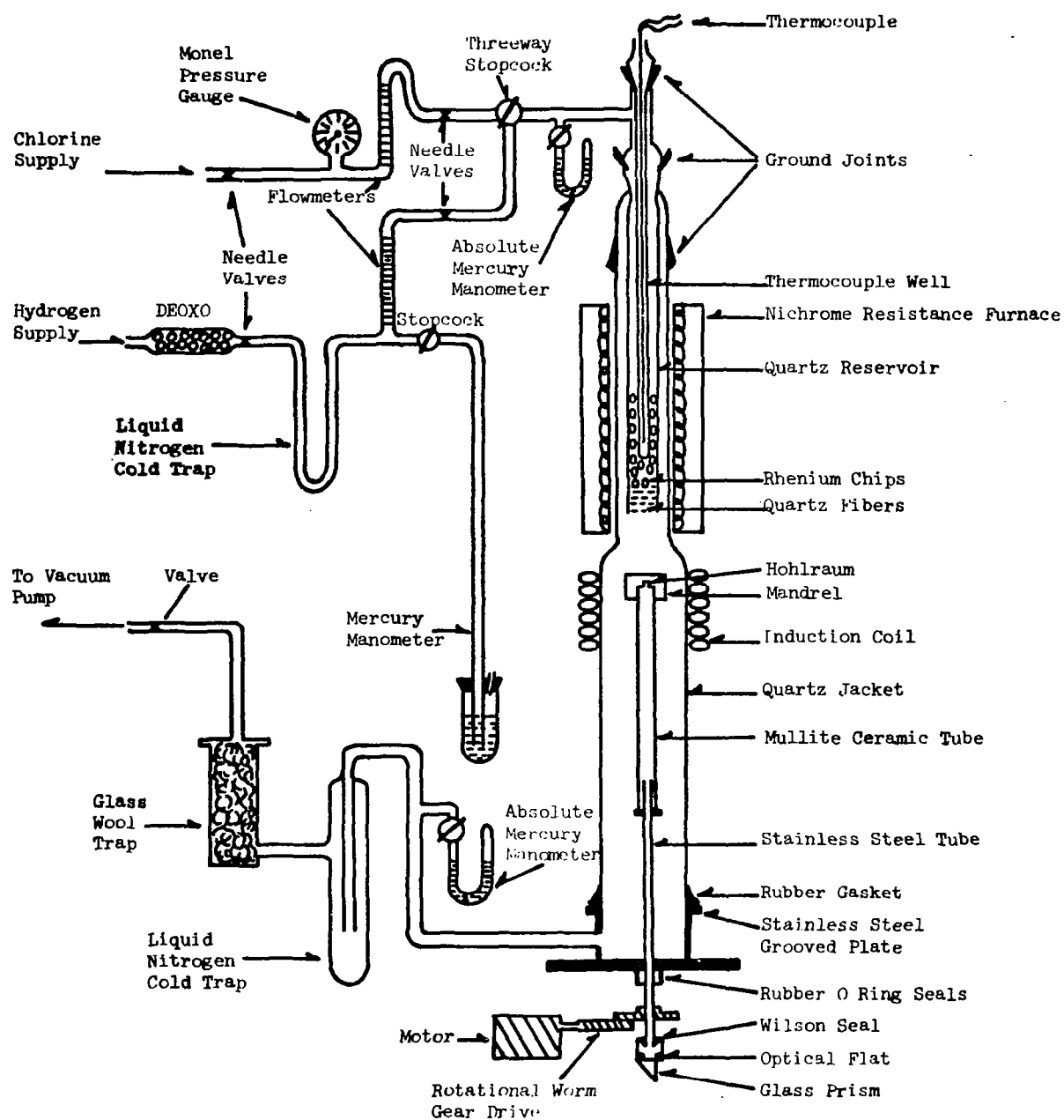


Fig. 1. Rhenium deposition apparatus

TABLE 1

IMPURITY CONTENTS OF RHENIUM POWDER PROCURED
FROM CLEVELAND REFRACTORY METALS

Element	Concentration (ppm)
C	38
O	2300
H	100
N	55
Mo	25
Si	<5
Mg	<1
Sn	<5
Cr	<5
Cu	<1
Ag	<1
W	<100
Al	<5
Ca	<1
Ni	<5
Fe	17
Na	<1
K	<1

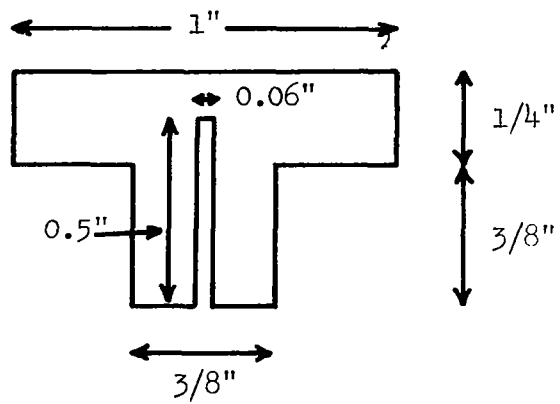


Fig. 2. Configuration and dimensions of molybdenum mandrel

temperature, rhenium pellet column height and the chlorination time. The amount of rhenium consumed by the chlorination reaction for each of the runs was less than 20% of the rhenium charge. The Cl/Re atom ratio was calculated from the weight of rhenium pellets reacted, the chlorine flow rate and the time of the run. The unreacted chlorine, as measured by a flowmeter located at the exit end of the deposition chamber (not shown in Fig. 1), was negligible in each case. The results shown in Table 2 indicate that Cl/Re atom ratios varying from 6.0 to 3.4 were obtained by varying the chlorination conditions, and that lower rhenium pellet temperature and higher chlorine flow rate favor the formation of chlorides of lower Cl/Re atom ratios.

2.3. DEPOSITION PROCEDURES

After the quartz reservoir was charged with about 400 grams of rhenium pellets, the deposition chamber was evacuated to remove air and moisture. The rhenium pellets were then baked at the chlorination temperature to be used for a few hours in flowing hydrogen to rid of any oxide present. After the pellets were cooled down in hydrogen, the molybdenum mandrel was installed in the deposition chamber and heated in flowing hydrogen for one hour at 1200°C to remove any oxide present on its surface. The chamber was then flushed with helium for one hour to remove the hydrogen. The temperature of the mandrel was then adjusted to the desired value before chlorine was admitted at the prescribed rate into the rhenium pellet reservoir to initiate the deposition operation. At the completion of the deposition the chlorine gas supply and the power supply to the chlorinator were turned off and the mandrel was cooled to room temperature in a helium atmosphere.

TABLE 2

Cl/Re ATOM RATIO OF THE CHLORINATION PRODUCT
FORMED UNDER VARIOUS CHLORINATION CONDITIONS

Chlorine Flow Rate* (c. c. /min.)	Rhenium Pellet Temperature (°C)	Rhenium Pellet Column Height (Inch)	Pressure Drop Across Rhenium Pellet Column (torr)	Time of Run (hrs.)	Cl/Re Atom Ratio
50	975	6	10	1	5.7
		4	10	3	5.8
	950	6	13	1	6.0
		6	14	3	5.7
		4	11	1	6.0
		4	11	3	6.1
	800	6	10	1	3.8
		6	10	3	3.8
		4	10	1	3.9
100	975	6	17	1	4.4
		4	15	2	4.7
	950	6	15	1	4.8
		4	15	2	4.7
150	975	6	24	1	4.3
		6	25	2	4.3
		4	22	1	4.2
	950	6	27	1	4.2
		6	25	2	4.3
		4	22	1	4.4
	800	6	20	1	3.4
		6	22	2	3.4

*For 1 atmosphere pressure and 25°C.

3. SAMPLE EVALUATION

All the samples prepared were analyzed for their impurity contents, microstructures and degree of (0001) preferred crystal orientation. For the determination of the degree of (0001) preferred crystal orientation, a disc of 0.600 inch diameter was cored from the sample by electrical-discharge-machining. The molybdenum substrate was then removed from the rhenium deposit by machining and grinding. The deposit surface was ground to 8 micro-inch finish, polished with emery paper and 0.5 micron diamond paste, and electropolished in a solution containing 350 c.c. of absolute alcohol, 175 c.c. of perchloric acid (density - 1.54 gm/c.c.) and 50 c.c. of butoxy ethanol at 2 amps/cm² and -10°C, using stainless steel as cathode. The distribution of the <0001> crystal axes in the deposit as a function of the tilt angle from the normal to the deposit surface was determined by X-rays, using a Norelco pole figure machine. The remnants from the electrical - discharge-machining operation were used to determine the impurity contents and the microstructures by chemical and metallographic techniques.

The electron vacuum work function of several planar rhenium discs were measured in a vacuum emission cell⁽⁴⁾ after the determination of their degrees of (0001) preferred crystal orientation. In the cell each sample was heated by electron bombardment to the desired temperature and the current-voltage relationship between the electropolished emitting surface and a water-cooled stainless steel collector-guard-ring assembly was measured

over the emitter surface temperature range of 1650-1850°C. The saturation emission current density I (amp/cm²) at zero field was obtained as a function of temperature. The Richardson work function " ϕ " and the pre-exponential factor " A " of the Richardson equation $I = AT^2 \exp(-\phi/kT)$ were deduced from the slope and the intercept of the plot of $\log I/T^2$ versus $1/T$, where k is the Boltzmann constant.

4. EVALUATION RESULTS

4.1. SCREENING STUDY

Ten screening runs were carried out to explore the effects of chlorine flow rate, molybdenum mandrel temperature and rhenium pellet temperature on the impurity contents, microstructures and degree of (0001) preferred crystal orientation in the deposit. Table 3 lists the deposition conditions and some of the evaluation results for these runs. It can be seen that the efficiency of deposition is higher at lower chlorine flow rate and higher mandrel temperature. Table 4 summarizes the impurity concentrations in these samples. Although these samples contain small amounts of interstitial impurities, the metallic impurity contents are very low. Figures 3(a) through (j) illustrate the microstructures of these samples. Low chlorine flow rate, high mandrel temperature and high rhenium pellet temperature favor the formation of porosity in the deposit. The porosities observed are mostly located at the grain boundaries of the deposit and seem to have been formed when neighboring

TABLE 3

DEPOSITION CONDITIONS AND RESULTS OF SCREENING DEPOSITION TESTS

Sample No.	Chlorine Flow Rate* (c. c. /min.)	Rhenium Pellet Temperature (°C)	Mandrel Temperature (°C)	Time of Run (hrs.)	Cl/Re Atom Ratio	Deposition Rate (mils/hr.)	Efficiency of Deposition** (%)	Degree of (0001) Orientation	Degree of Porosity in Deposit
10-D	150	975	1100	5	4.2	7.5	26	medium	none
2-D	150	975	1200	3	4.1	12.7	37	strong	high
9-D	150	975	1300	3	4.1	20.3	50	medium	medium
8-D	150	800	1100	4	3.7	8.3	21	medium	very low
3-D	150	800	1200	4	3.9	12.5	32	strong	very low
4-D	150	800	1300	4	3.7	20.8	50	weak	medium
1-D	50	975	1200	3	5.7	5.7	56	medium	high
7-D	50	800	1100	7	3.9	6.6	40	medium	medium
6-D	50	800	1200	6.5	3.8	7.0	48	weak	very high
5-D	50	800	1300	5	3.8	7.4	55	very weak	none

* For 1 atmosphere pressure and 25°C

** $\frac{\text{Weight of rhenium deposited on mandrel}}{\text{Weight of rhenium pellet used}}$

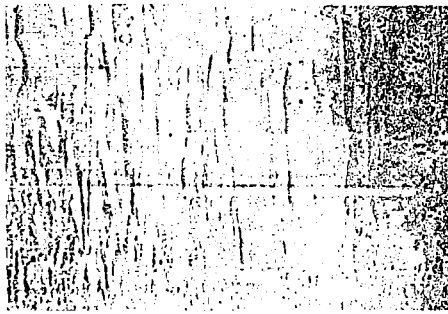
Note: Rhenium pellet column height was 6-1/2 inches in all cases.
Chlorine pressure drop across rhenium pellet column was between 26 to 32 torr for 150 c. c. /min. flow rate and 4 to 8 torr for 50 c. c. /min. flow rate. Chlorine pressure in deposition chamber was less than 1 torr.

TABLE 4

IMPURITY CONTENTS IN RHENIUM SAMPLES
FOR SCREENING STUDY

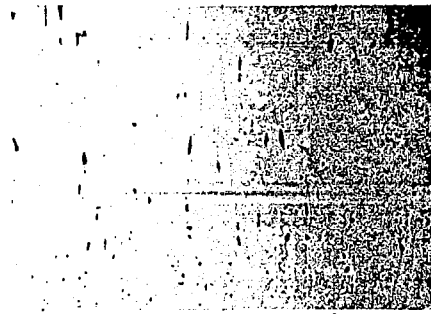
Elements Determine in ppm	Sample No. 1D	Sample No. 2D	Sample No. 3D	Sample No. 4D	Sample No. 5D	Sample No. 6D	Sample No. 7D	Sample No. 8D	Sample No. 9D	Sample No. 10D
C	53	55	20	23	61	63	46	35	20	30
O	50	45	12	25	47	45	34	25	15	25
N	20	30	20	20	30	29	20	30	20	25
Na	<1	<1	<1	5	3	<1	<1	<1	<1	<1

Other impurities (in ppm) : Cl < 10, Ag < 1, Al < 5, Ca < 1, Cr < 5,
Cu < 1, Fe < 5, Mg < 1, Mo < 10, Sn < 5,
W < 100, K < 5



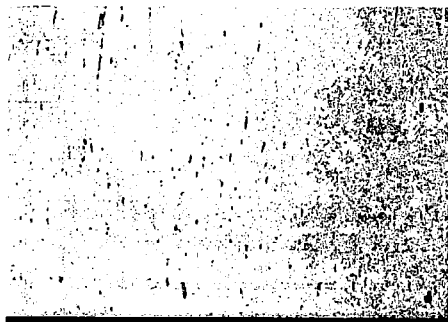
M 33939-1

(a) Sample 10-D (150/975/1100)



M 33511-1

(b) Sample 2-D (150/975/1200)



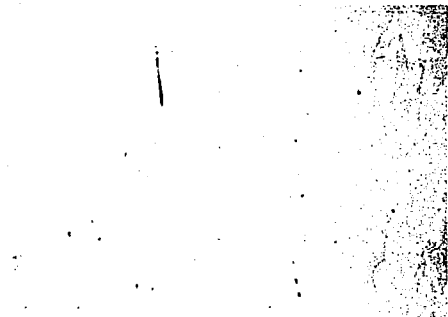
M 33878-1

(c) Sample 9-D (150/975/1300)



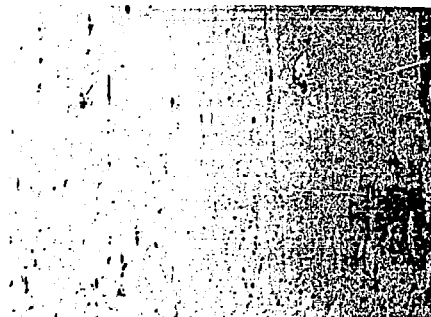
M 33773-1

(d) Sample 8-D (150/800/1100)



M 33512-1

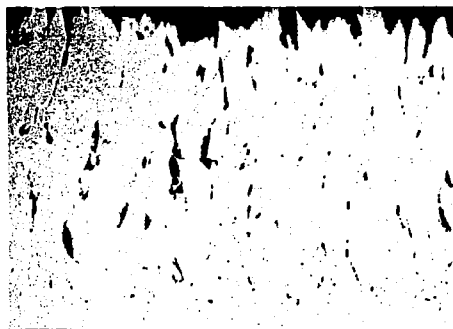
(e) Sample 3-D (150/800/1200)



M 33514-1

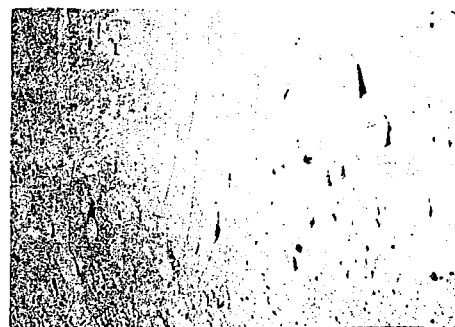
(f) Sample 4-D (150/800/1300)

Fig. 3. Microstructures of CVD rhenium samples for screening study. The numbers shown in parentheses beside each sample designation are chlorine flow rate in standard c. c. /min., rhenium pellet temperature in °C, and mandrel temperature in °C. (Sheet 1 of 2) Note: $\leftarrow 10 \text{ mil} \rightarrow$



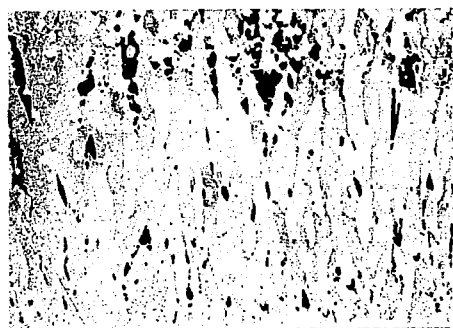
M 33510-1

(g) Sample 1-D (50/975/1200)



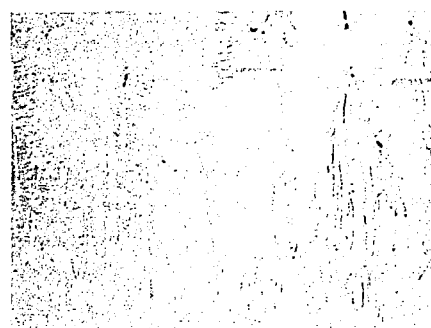
M 33516-1

(h) Sample 7-D (50/800/1100)



M 33515-1

(i) Sample 6-D (50/800/1200)



M 33514-1

(j) Sample 5-D (50/800/1300)

Fig. 3. Microstructures of CVD rhenium samples for screening study. The numbers shown in parentheses beside each sample designation are chlorine flow rate in standard c. c. / min. , rhenium pellet temperature in °C, and mandrel temperature in °C. (Sheet 2 of 2) Note: ←10 mil→

crystal grains grew into each other and trapped voids in between them. No correlation between the degree of porosity and the impurity concentrations in the deposits could be established. Figure 4 shows the distributions of the $\langle 0001 \rangle$ crystal axes in the ten screening test samples. Better (0001) oriented deposits, such as 2-D and 3-D, which were prepared at a chlorine flow rate of 150 c. c. /min and a mandrel temperature of 1200°C , are indicated by the presence of more $\langle 0001 \rangle$ crystal axes in the vicinity of the normal to the deposit surface. Thus the screening test results indicate that higher chlorine flow rate (150 c. c. /min. versus 50 c. c. /min.), lower rhenium pellet temperature (800°C versus 975°C) and a mandrel temperature of 1200°C are favored for the preparation of rhenium deposits having a high degree of (0001) preferred crystal orientation and low porosity.

4.2. OPTIMIZATION STUDY

Ten more test samples were prepared in order to determine whether the degree of (0001) preferred crystal orientation achieved in the screening studies could be improved by modifying the deposition conditions using the guidelines established in the screening tests. Chlorine flow rates from 100 c. c. /min. to 250 c. c. /min., rhenium pellet temperature down to 700°C and mandrel temperatures between 1150°C to 1250°C were investigated for their effects on impurity contents, microstructures, and degree of (0001) preferred crystal orientation of the rhenium deposits prepared. The deposition conditions and some of the test results are summarized in Table 5. These deposits were porosity free except Samples 16-D and 20-D which were deposited at mandrel temperatures higher than 1200°C . Figure 5 shows the typical microstructures

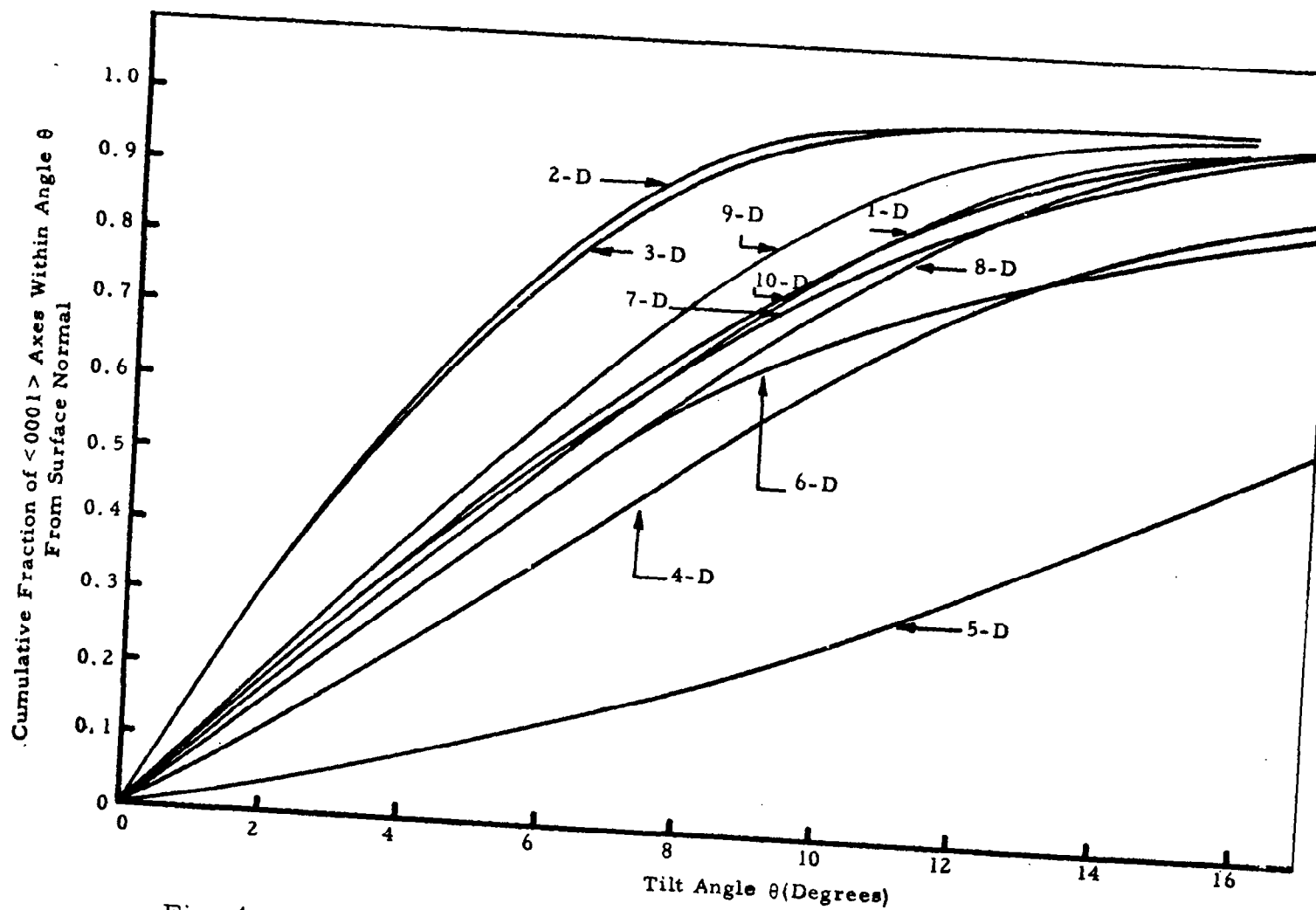


Fig. 4. Distribution of the $\langle 0001 \rangle$ axes in ten rhenium screening study samples

TABLE 5

DEPOSITION CONDITIONS AND RESULTS OF OPTIMIZATION DEPOSITION TESTS

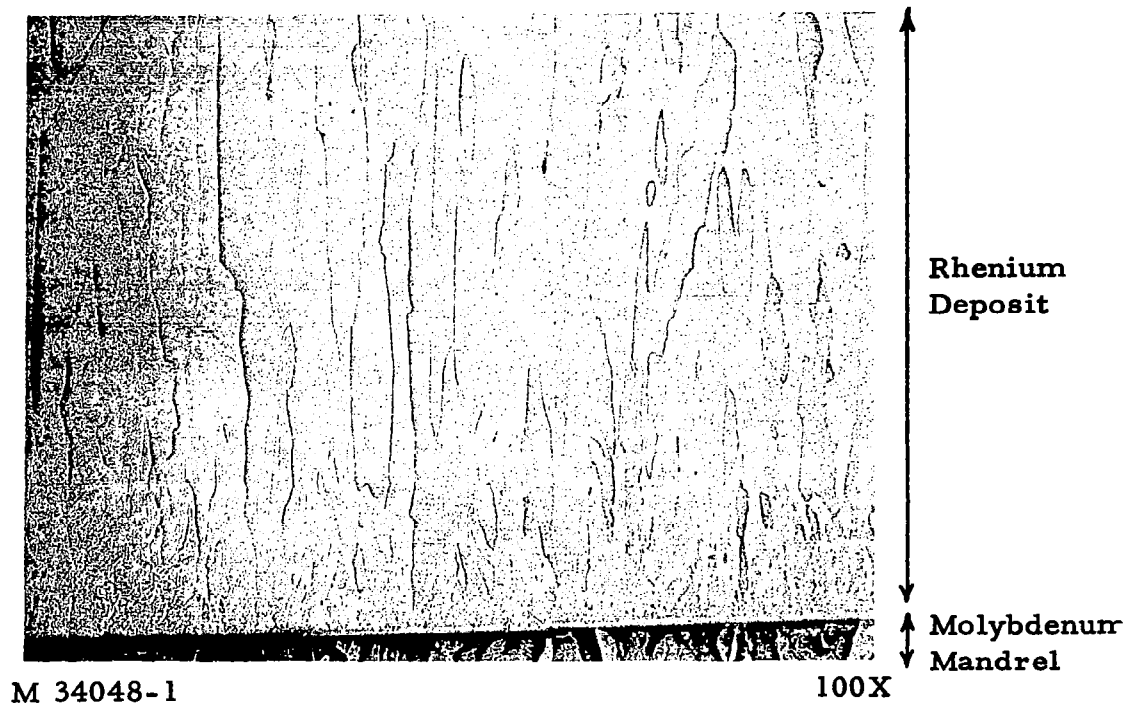
Sample No.	Chlorine Flow Rate* (c. c. /min.)	Rhenium Pellet Temperature (°C)	Mandrel Temperature (°C)	Time of Run (hrs.)	Cl/Re Atom Ratio	Deposition Rate (mils/hr.)	Efficiency of Deposition** (%)	Degree of (0001) Orientation	Degree of Porosity in Deposit
11-D	100	800	1200	5	3.6	11.2	48	medium	none
12-D	150	700	1200	4	6.0	8.2	36	medium	none
13-D	150	800	1150	4	3.6	11	29	medium	none
14-D	100	800	1150	5.2	3.7	7.6	31	medium	none
15-D	200	800	1200	3.5	3.6	14.9	28	strong	none
16-D	100	800	1250	4	3.5	13.2	49	strong	medium
17-D	250	800	1200	3.25	3.8	17.5	27	medium strong	none
20-D	200	800	1225	3-1/2	3.6	22.3	29	strong	medium
21-D	200	800	1175	3-1/2	3.7	10.9	25	medium strong	none
22-D	225	800	1175	3.75	4.0	14.1	25	medium strong	none

*For 1 atmosphere pressure and 25°C

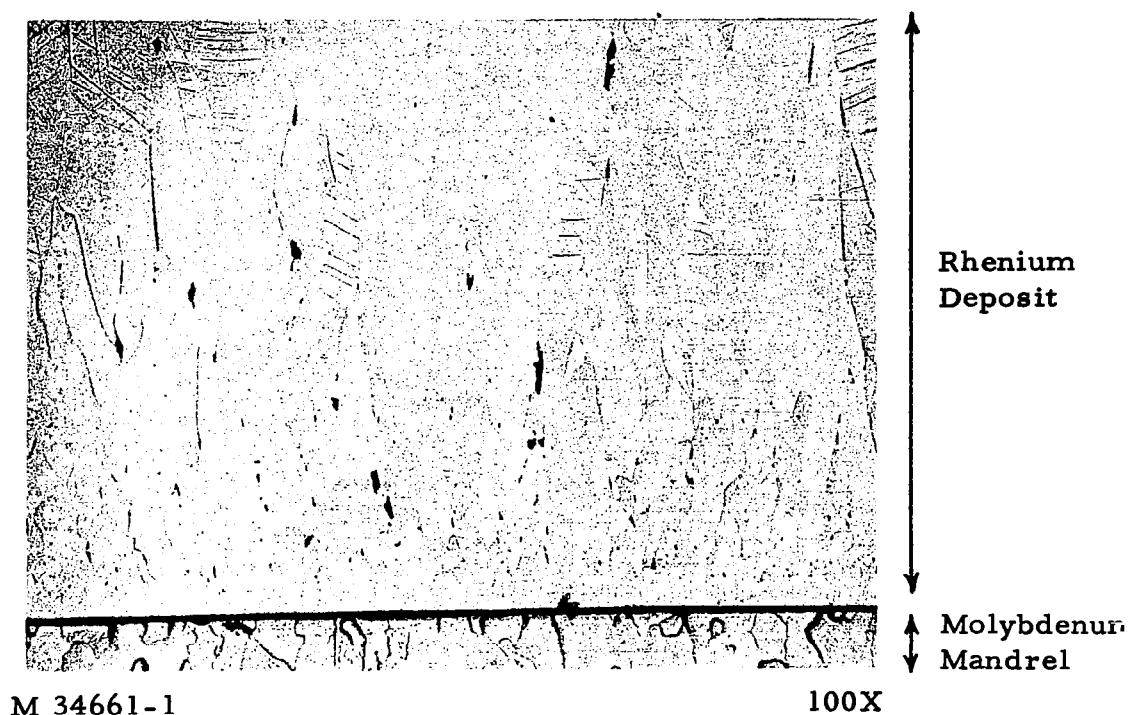
**Weight of rhenium deposited on mandrel
Weight of rhenium pellets used

Note: Rhenium pellet colum height was 7-1/2 inches in all cases.

Chlorine pressure drop across rhenium pellet column was 45 torr for 250 c. c. /min. and 225 c. c. /min. flow rates, 40 torr for 200 c. c. /min. flow rate, 27-30 torr for 150 c. c. /min. flow rate and 12-15 torr for 100 c. c. /min. flow rate. Chlorine pressure in deposition chamber was less than 1 torr.



(a) Sample 15-D (200/800/1200)
Porosity-free deposit



(b) Sample 20-D (200/800/1225)
Presence of porosities in deposit

Fig. 5. Microstructures of some CVD rhenium samples for optimization study. The numbers shown in parentheses beside each sample designation are chlorine flow rate in standard c. c. /min., rhenium pellet temperature in °C, and mandrel temperature in °C. Note: $\leftarrow 10 \text{ mil} \rightarrow$

of a porosity-free deposit (Sample 15-D) and that of a deposit containing porosity (Sample 20-D). Table 6 lists the impurity contents in these deposits. Figure 6 shows the distribution of the $\langle 0001 \rangle$ crystal axes in these samples. These results and those shown in Table 3 for the screening studies were used to define the optimum deposition conditions. A chlorine flow rate of 200 c. c. /min. yielded rhenium deposits of a higher degree of (0001) preferred crystal orientation than chlorine flow rates of 100 c. c. /min., 150 c. c. /min., and 250 c. c. /min. (compare Sample 15-D with Samples 11-D, 3-D, and 17-D). A rhenium pellet temperature of 800°C seems to be a better choice than either 975°C or 700°C , since a sample prepared at a rhenium pellet temperature of 975°C contained a large amount of porosity (compare Sample 2-D with Sample 3-D) and a sample prepared at a rhenium pellet temperature of 700°C was not as well oriented as a sample prepared at a rhenium pellet temperature of 800°C (compare Sample 12-D with Sample 3-D). A mandrel temperature of 1200°C represents the optimum value, since deposits prepared at mandrel temperatures of 1225°C and 1250°C contain porosities at grain boundaries (compare Sample 15-D with Samples 17-D and 20-D), and a deposit prepared at a mandrel temperature of 1175°C was not as well oriented as a deposit prepared at a mandrel temperature of 1200°C (compare Sample 21-D with Sample 15-D). Thus the optimum choices of the deposition conditions for obtaining porosity-free rhenium deposited of strong (0001) preferred crystal orientation are: chlorine flow rate, 200 c. c. /min., rhenium pellet temperature, 800°C , and mandrel temperature, 1200°C .

TABLE 6

IMPURITY CONTENTS IN RHENIUM SAMPLES
FOR OPTIMIZATION STUDY

Elements Determined in ppm	Sample No. 11-D	Sample No. 12-D	Sample No. 13-D	Sample No. 14-D	Sample No. 15-D	Sample No. 16-D	Sample No. 17-D	Sample No. 20-D	Sample No. 21-D	Sample No. 22-D
C	12	18	13	25	9	21	15	15	10	12
O	25	32	48	42	32	25	28	25	35	20
N	4	3	4	5	4	3	3	3	3	3
Al	30	25	<5	<5	<5	<5	<5	<5	<5	<5
Ca	1	2	1	1	2	3	1	2	1	1
Na	3	5	2	2	2	2	2	2	2	2

Other impurities 9in ppm): Cl < 1, Ag < 1, Cr < 5, Cu < 1,
Fe < 5, Mg < 1, Mo < 10, Ni < 5,
Si < 5, Sn < 5, W < 100, K < 5.

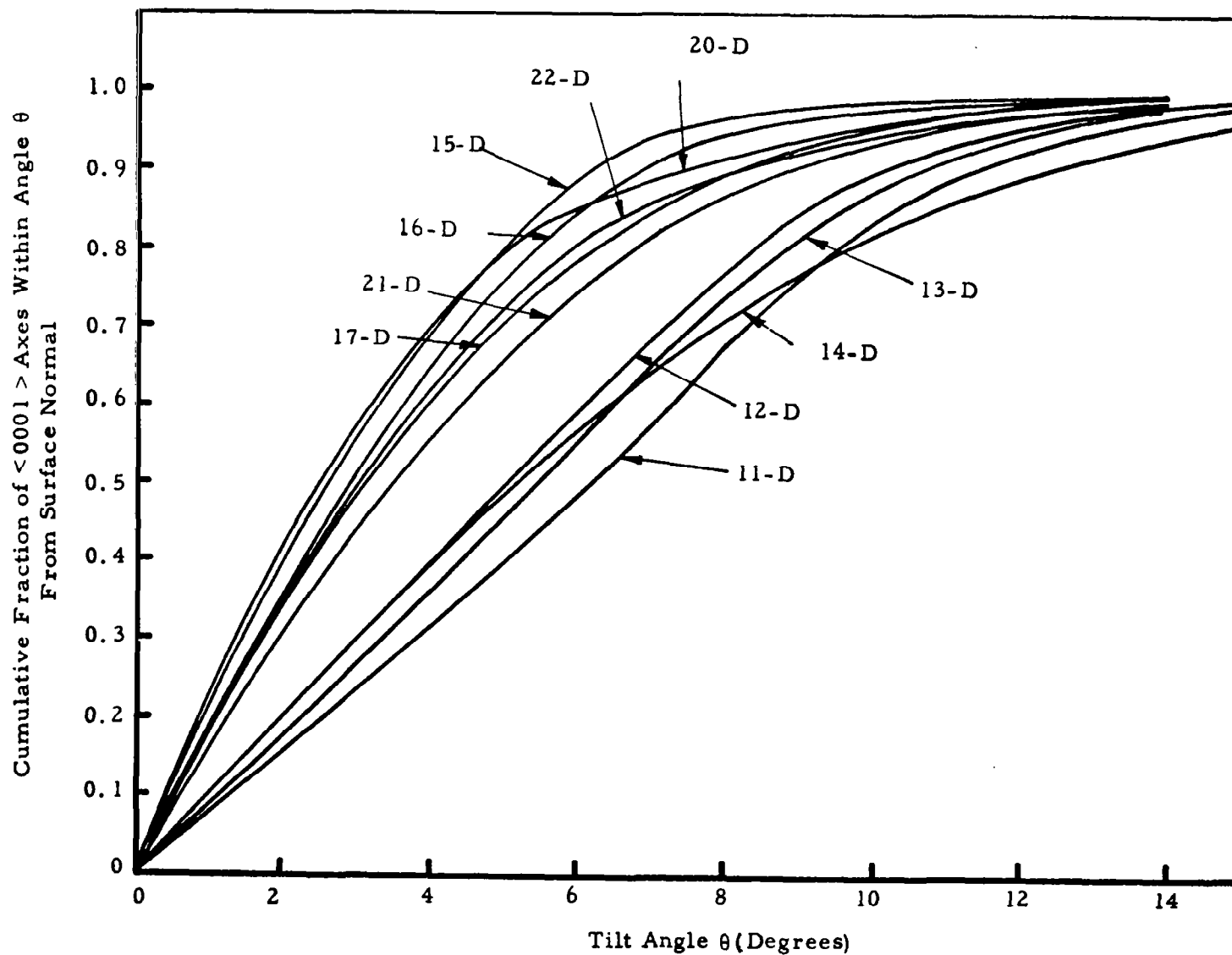


Fig. 6. Distributions of the $\langle 0001 \rangle$ axes in ten rhenium optimization study samples

Seven of the optimization study samples were outgassed at 1830°C for 50 hours and their vacuum emission characteristics were monitored in the temperature range 1650-1850°C for 250 hours. The Richardson work functions " ϕ " and the pre-exponential "A" values deduced from these results are given in Table 7 together with the tilt angle θ within which 90% of the $\langle 0001 \rangle$ crystal axes scanned by the X-ray beam are located. These results indicate that higher ϕ values are associated with lower θ values and that a work function of 5.19 eV was achieved with the best oriented Sample 15-D. Since θ values can be determined readily by X-ray means, this established relationship should be useful for screening rhenium emitters for thermionic conversion application.

4.3. REPRODUCIBILITY STUDIES

Five samples, 23-D through 27-D, were prepared under the same conditions as used for the preparation of the best oriented Sample 15-D during the optimization study, i. e. a chlorine flow rate of 200 c. c. /min., a rhenium pellet temperature of 800°C and a mandrel temperature of 1200°C. The impurity contents and the microstructures of these samples were found to be similar to that of Sample 15-D. Figure 7 shows the distribution of the $\langle 0001 \rangle$ axes in these samples and Table 8 summarizes the vacuum emission study results together with the tilt angle θ within which 90% of the $\langle 0001 \rangle$ crystal axes scanned by the X-ray beam are located. Sample 23-D is slightly better oriented and accordingly has a slightly higher work function. The other four samples have essentially the same θ and ϕ values which do not differ significantly from

TABLE 7

VACUUM EMISSION RESULTS FOR SEVEN
OPTIMIZATION STUDY SAMPLES

Sample Designation	Pre-Exponential Factor A (amp/cm ² /°K ²)	Richardson Work Function (eV)	Angle From Surface Normal Within Which 90% of <0001> Axes Scanned by X-ray Beam are Located
14-D	162	4.79	14°
15-D	191	5.19	6.5°
16-D	173	5.10	7.5°
17-D	130	5.02	8°
20-D	209	5.12	7°
21-D	101	5.00	8.5°
22-D	143	5.05	8°

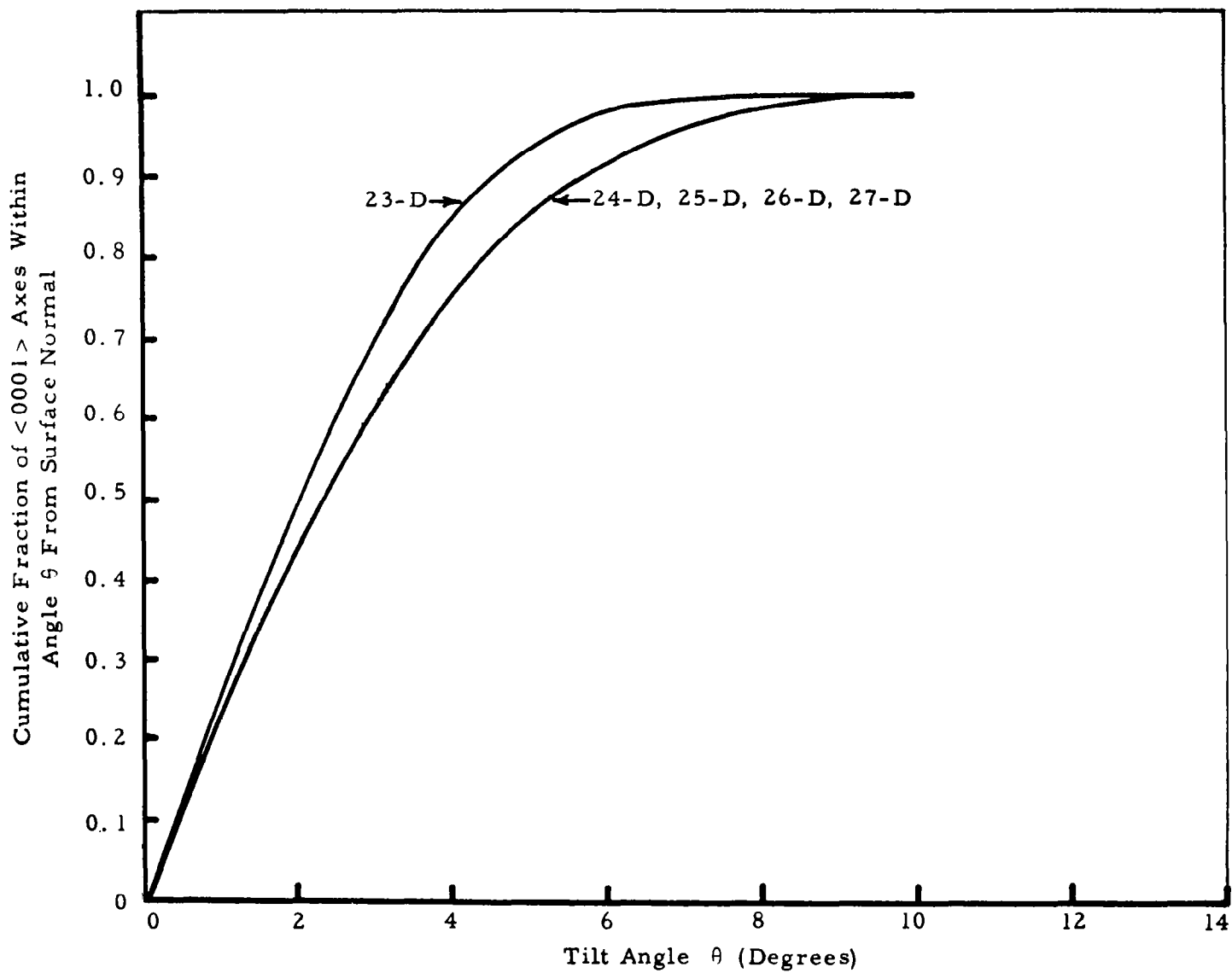


Fig. 7. Distribution of the $\langle 0001 \rangle$ axes in five rhenium reproducibility study samples

TABLE 8

VACUUM EMISSION RESULTS FOR FIVE
REPRODUCIBILITY STUDY SAMPLES

Sample Designation	Pre-Exponential Factor A amp/cm ² /°K ²	Richardson Work Function (eV)	Angle From Surface Normal Within Which 90% of <0001> Axes Scanned by X-ray Beam are Located
23-D	97	5.26	4.5°
24-D	126	5.19	5.7°
25-D	104	5.18	5.7°
26-D	95	5.22	5.7°
27-D	98	5.17	5.7°

from that of Sample 15-D. These results indicate that (0001) oriented rhenium emitters of vacuum work functions as high as 5.2 eV can be reproducibly prepared by chemical vapor deposition under the conditions defined in this study.

5. PREPARATION OF CYLINDRICAL RHENIUM EMITTERS

Three cylindrical rhenium emitters were prepared by depositing rhenium on tantalum mandrels supplied by NASA. These mandrels were 4.6 inch in length and had an outside diameter of 0.862 inch and an inside diameter of about 0.7 inch.

In order to improve the uniformity of the as-deposited thickness of the rhenium layer over the entire emitting length, the deposition apparatus shown in Fig. 1 was modified in two respects. First, the rhenium chloride generator was moved from the top of the deposition chamber to its side so that the rhenium chloride vapor entered the deposition chamber in a direction perpendicular rather than parallel to the cylindrical axis of the mandrel. Secondly, in addition to the rotary motion (2 r. p. m.), the mandrel was also moved axially across the rhenium chloride vapor beam during the deposition. The results obtained in several trial runs showed that rhenium layer of uniform thickness and strong (0001) preferred crystal orientation could be deposited over the entire 4.6 inch mandrel length at a rate of 4 to 5 mils per hour under the same deposition conditions as that used for the preparation of Sample 15-D.

Figures 8, 9, and 10 show the distribution of the $\langle 0001 \rangle$ crystal axes in the three as-deposited emitters. It can be seen that 90% of the $\langle 0001 \rangle$ crystal axes scanned by the X-ray beam lying within 5° to 6° from the normal of the emitting surfaces. On the basis of the results shown in Table 8, it is concluded that these emitters should possess vacuum work functions of about 5.2 eV.

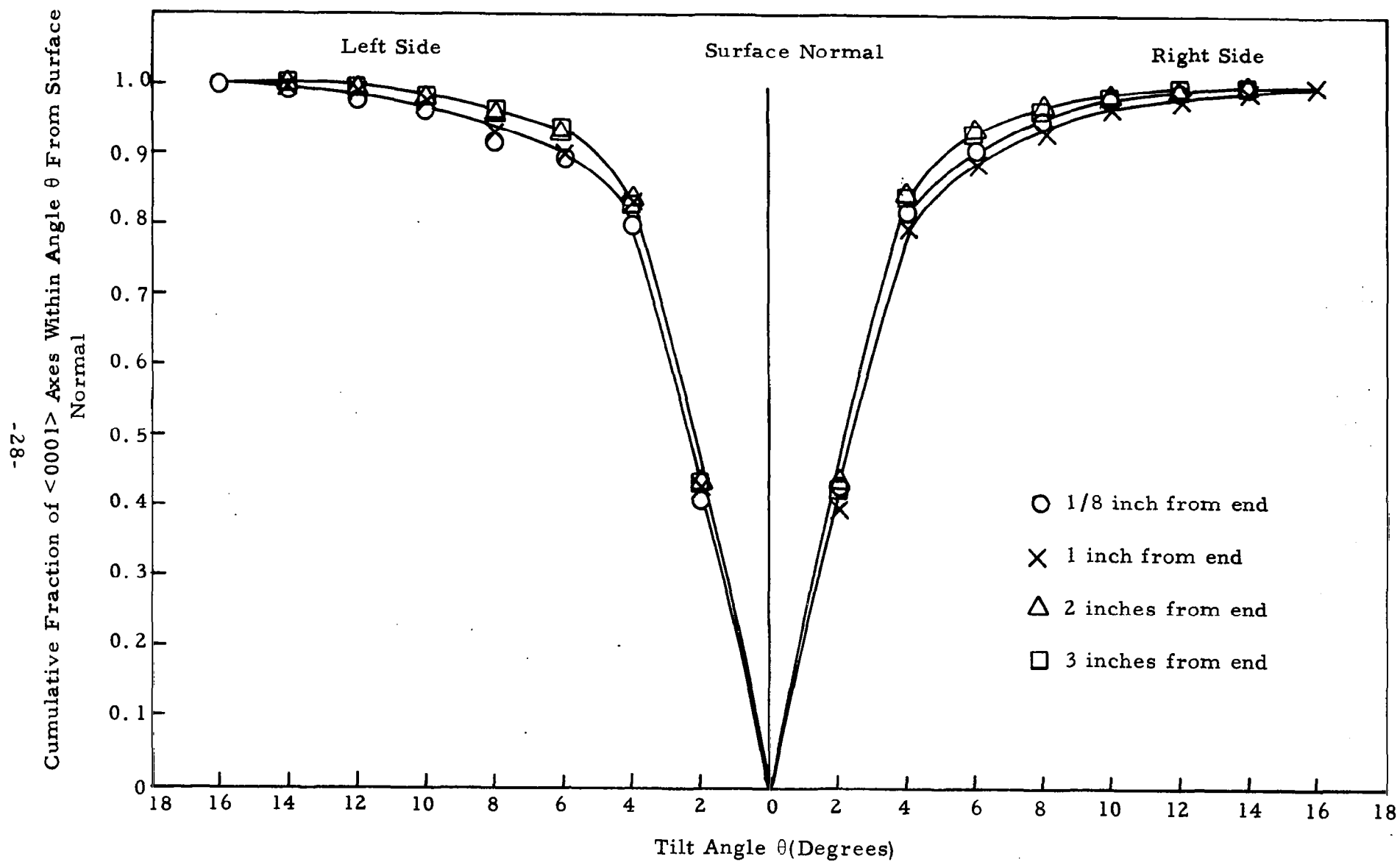


Fig. 8. Distribution of the $\langle 0001 \rangle$ axes in as-deposited cylindrical rhenium emitter No. 1

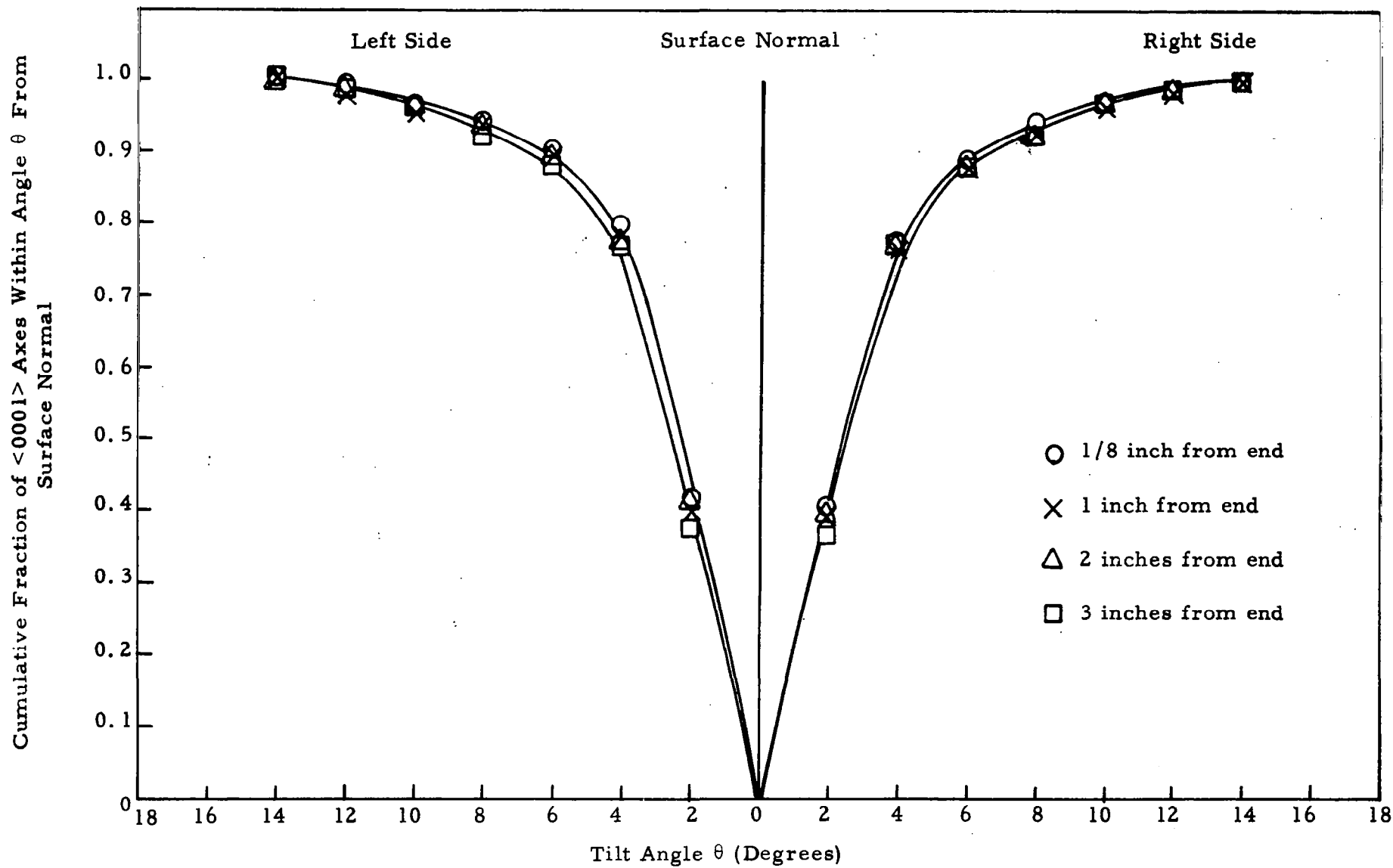


Fig. 9. Distribution of the $\langle 0001 \rangle$ axes in cylindrical rhenium emitter No. 2

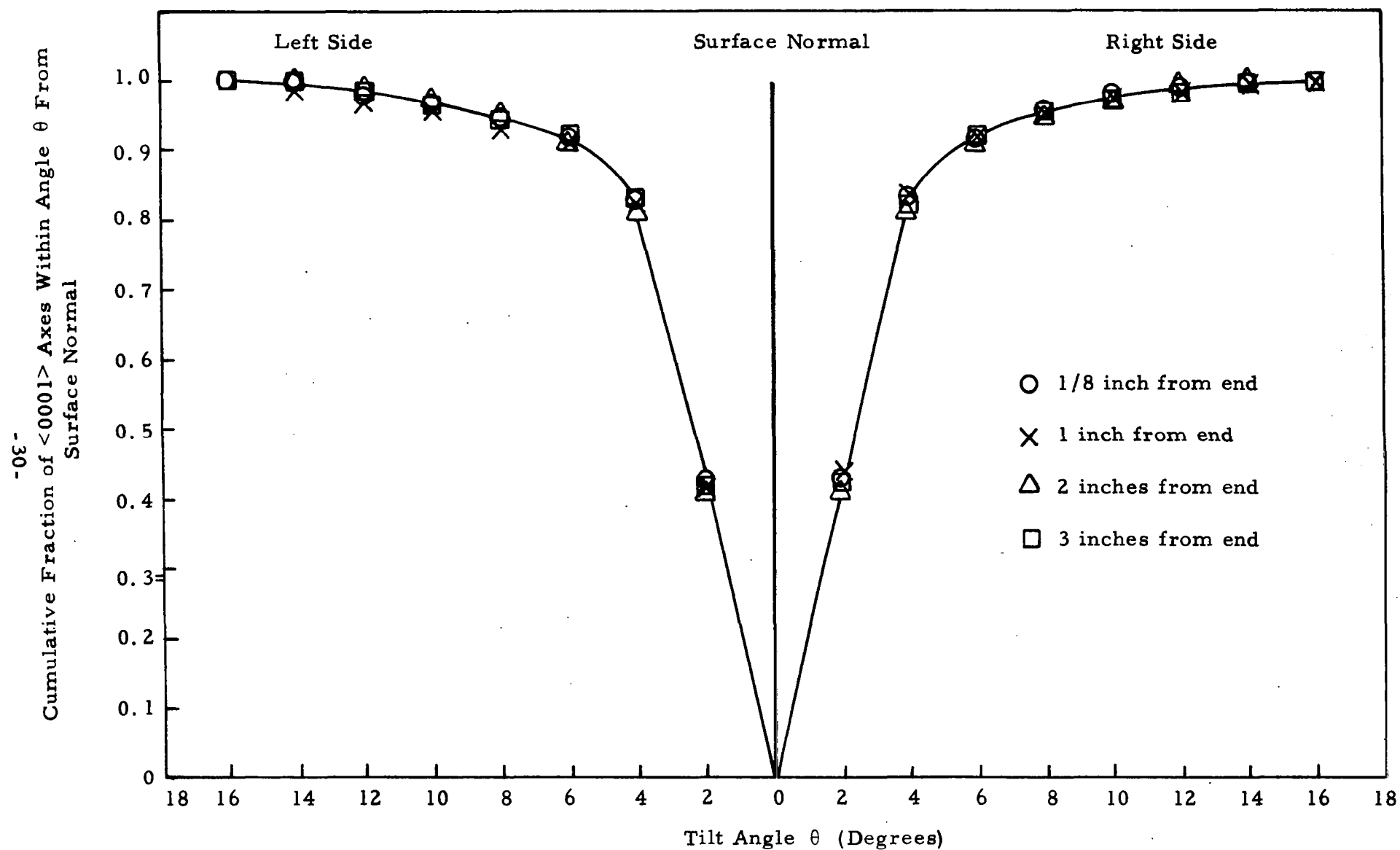


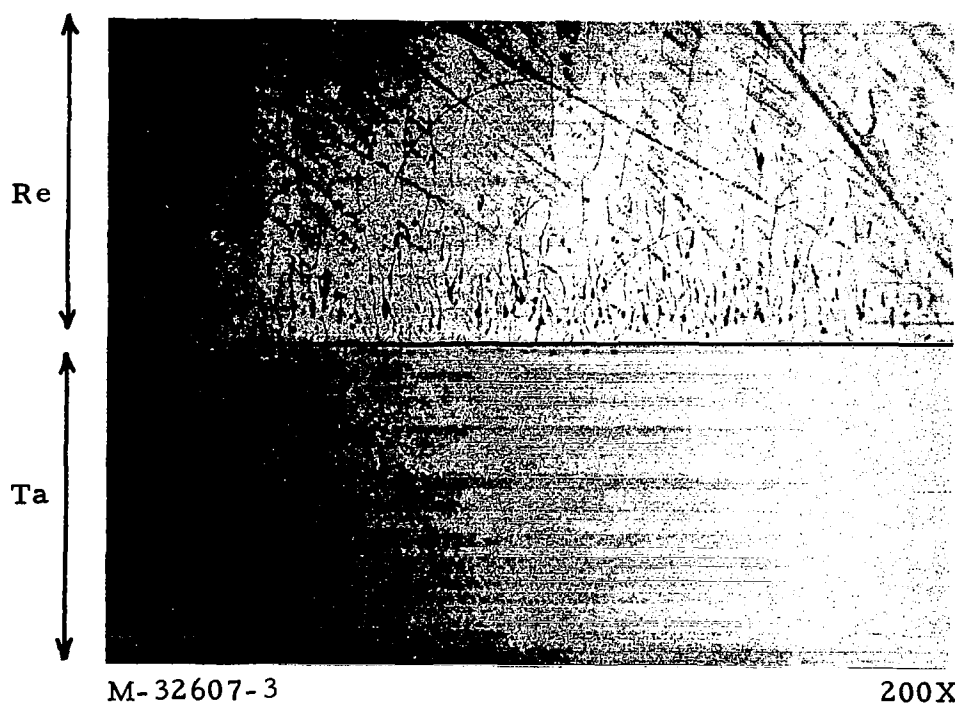
Fig. 10. Distribution of the $\langle 0001 \rangle$ axes in cylindrical rhenium emitter No. 3

APPENDIX A. INTERDIFFUSION BETWEEN RHENIUM AND TANTALUM AT 1500°C

To assess the long-term thermal and mechanical stability of the interface between the rhenium emitting layer and the tantalum substrate at a design operating temperature of 1500°C, diffusion couples of CVD rhenium on tantalum were prepared and annealed in vacuum (10^{-6} torr) at 1500°C for 100 and 1000 hours. The annealed couples were sectioned and the microstructures and composition distributions across the interface were studied metallographically and by electron microprobe analysis. The results are shown in Figs. 11 and 12. The width of the diffusion zone was found to be about 6 microns after 100 hours at 1500°C. A second phase of about 2 micron thickness and containing about 18% tantalum was also detected. Some Kirkendall voids were present on the tantalum side of the interface. After a diffusion time of 1000 hours at 1500°C, the thicknesses of the diffusion zone and the second phase grew to 20 microns and 4 microns respectively. Kirkendall voids, porosities and some cracks were observed in the diffusion zone. It appears that because of the interdiffusion and the formation of a second phase at the interface, the long-term thermal and mechanically stability of rhenium emitters deposited on tantalum substrates is questionable.



- (a) Unetched. Good bond, some Kirkendall voids in Ta next to Re. Porosity in Re next to Ta. Diffusion zone width ~ 6 microns. Presence of zone of second phase ($\sim 18\%$ Ta) of 2 micron width in diffusion zone.

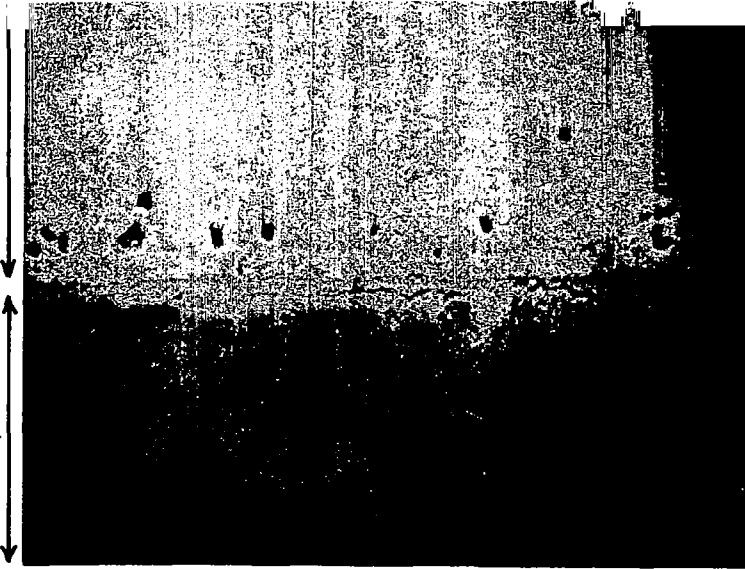


- (b) Etched. The dark line at the interface is due to selective etching of the diffusion zone

Fig. 11. Ta-Re interface after 100 hours at 1500°C

Re

Ta



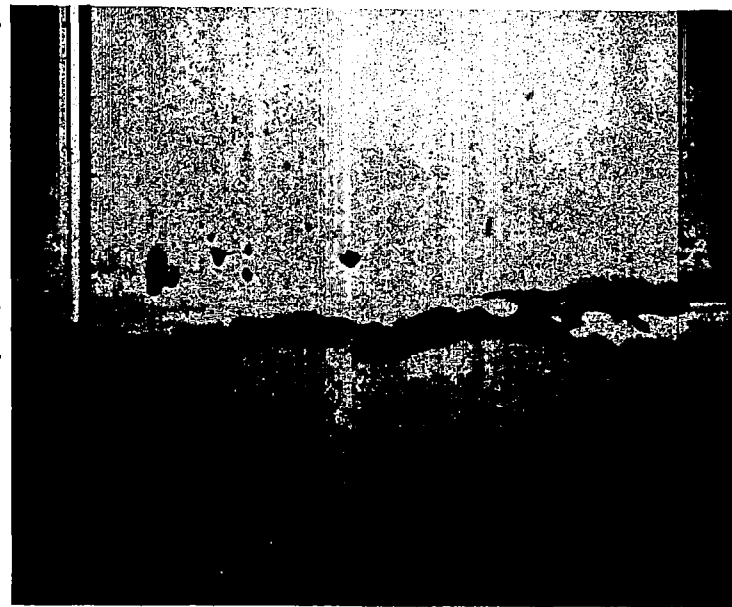
M-33211-4

650X

(a) Unetched. Diffusion zone with some porosities in rhenium and Kirkendall voids in Ta. Width of diffusion zone ~20 microns. Presence of zone of second phase (15-20% Ta) of ~4 micron width in diffusion zone

Re

Ta



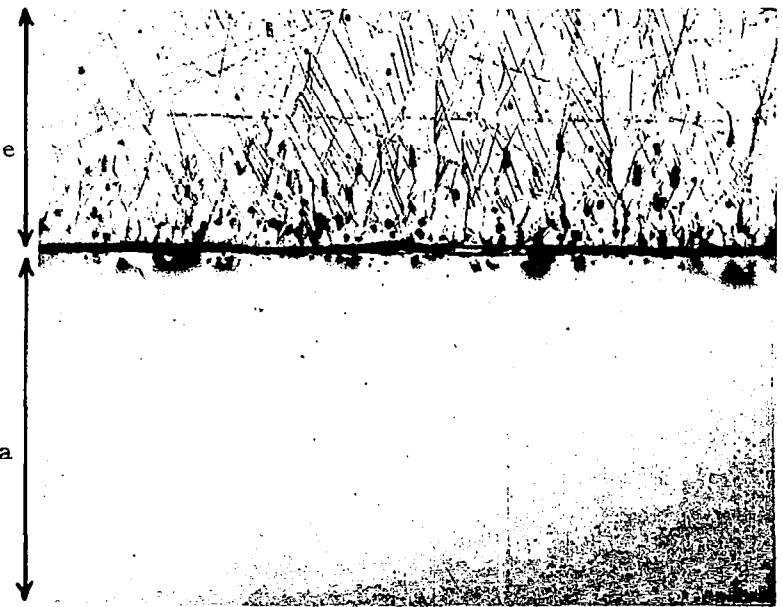
M-33211-2

650X

(b) Unetched. Diffusion zone containing cracks

Re

Ta



M-33315-1

200X

(c) Etched

Fig. 12. Ta-Re interface after 1000 hours at 1500°C

APPENDIX B. PREPARATION OF TWELVE CHLORIDE-FLUORIDE DUPLEX TUNGSTEN EMITTERS

At NASA's request, the workscope of this contract was extended to including the preparation of twelve cylindrical chloride-fluoride duplex tungsten emitters. The dimensions of these emitters are as follows.

O. D. 1.100 ± 0.0005 inch

I. D. 1.02 ± 0.0005 inch

Length 4.07 ± 0.001 inch

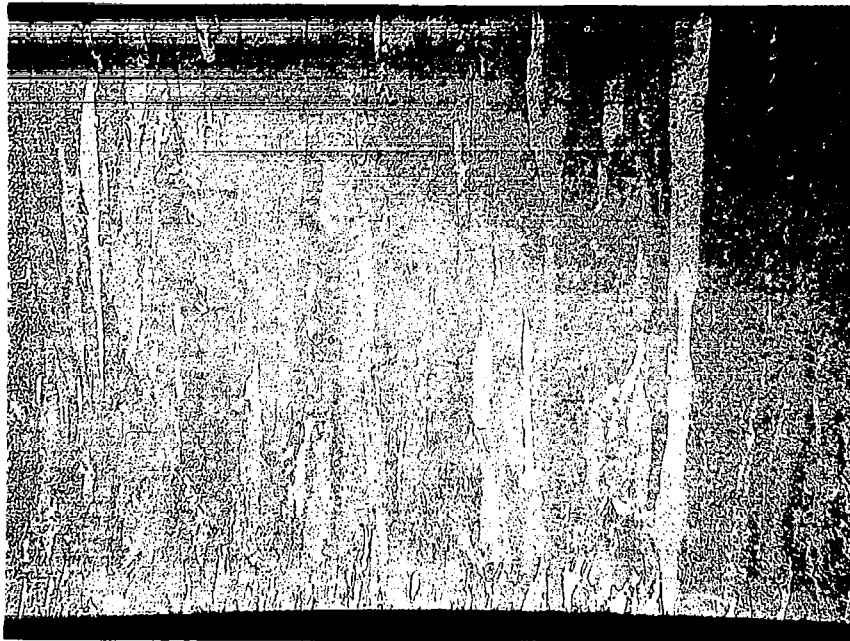
Thickness of fluoride (WF_6)tungsten* substrate 0.030 inch

Thickness of chloride tungsten** emitting layer 0.010 inch

The fluoride tungsten substrate was deposited on a molybdenum mandrel at a mandrel temperature of 580°C , a hydrogen flow rate of 2000 c. c. /min., and a WF_6 flow rate of 350 c. c. /min. The total gas pressure in the deposition chamber was 130 torr. Prior to the deposition, the mandrel was outgassed in vacuum (10^{-7} torr) at 1000°C for 2 hours. Figure 13 shows the typical microstructures of the deposit, and Table 9 lists the impurity contents of the twelve

*Prepared by the hydrogen reduction of tungsten hexafluoride

**Prepared by the hydrogen reduction of tungsten chlorides



M 38155-1

75X

Fig. 13. Typical microstructures of the fluoride tungsten substrate after outgassing in vacuum at 1800°C for 12 hours. 10 mils

TABLE 9

IMPURITY CONTENTS OF FLUORIDE
TUNGSTEN SUBSTRATES

Sample No.	Impurity Contents (ppm)			
	F	O	N	C
1	5	3	<1	5
2	7	2	<1	8
3	5	2	<1	6
4	10	5	<1	5
5	8	3	<1	8
6	6	1	<1	5
7	7	3	<1	4
8	7	6	<1	2
9	5	4	<1	4
10	5	7	<1	5
11				
12				

fluoride tungsten substrates after the removal of the molybdenum mandrel by acid etching and outgassing in vacuum (10^{-7} torr) at 1800°C for 12 hours. These impurity contents fall within the ranges specified for thermionic application.

Each fluoride tungsten substrate was ground to a diameter of 1.080 inch and a surface finish of 8 microinch, degreased and annealed in vacuum (10^{-7} torr) at 1800°C for 4 hours. Prior to the deposition of the chloride tungsten emitting layer, the fluoride tungsten surface was cleaned in hydrogen at 1100°C for 1 hour in the deposition chamber. Deposition of the chloride tungsten was carried out at a substrate temperature of 1100°C , a hydrogen flow rate of 275 c. c. /min., a chlorine flow rate of 260 c. c. /min., and a tungsten chip temperature of 850°C . The total gas pressure in the deposition chamber was 7 torr.

Each chloride-fluoride duplex tungsten emitter thus prepared was annealed at 1000°C for 2 hours and then ground and polished with silicon carbide paper and 0.5 micron diamond paste to a diameter of 1.102 inch. This was followed by electropolishing in 1% KOH solution to the required diameter of 1.100 inch and cutting to the specified length (4.07 inch). Each finished emitter was heated at 1627°C for 12 hours in vacuum (10^{-7} torr) to stabilize the grain structures. The distributions of the $\langle 110 \rangle$ crystal axes in each emitter was then determined by X-rays. The results shown in Fig. 14 indicate that 90% of the $\langle 110 \rangle$ crystal axes scanned by the X-rays fall within 6° to 9° from the normal to the emitting surfaces. On the basis of previous correlation⁽⁵⁾ between the degree of (110)

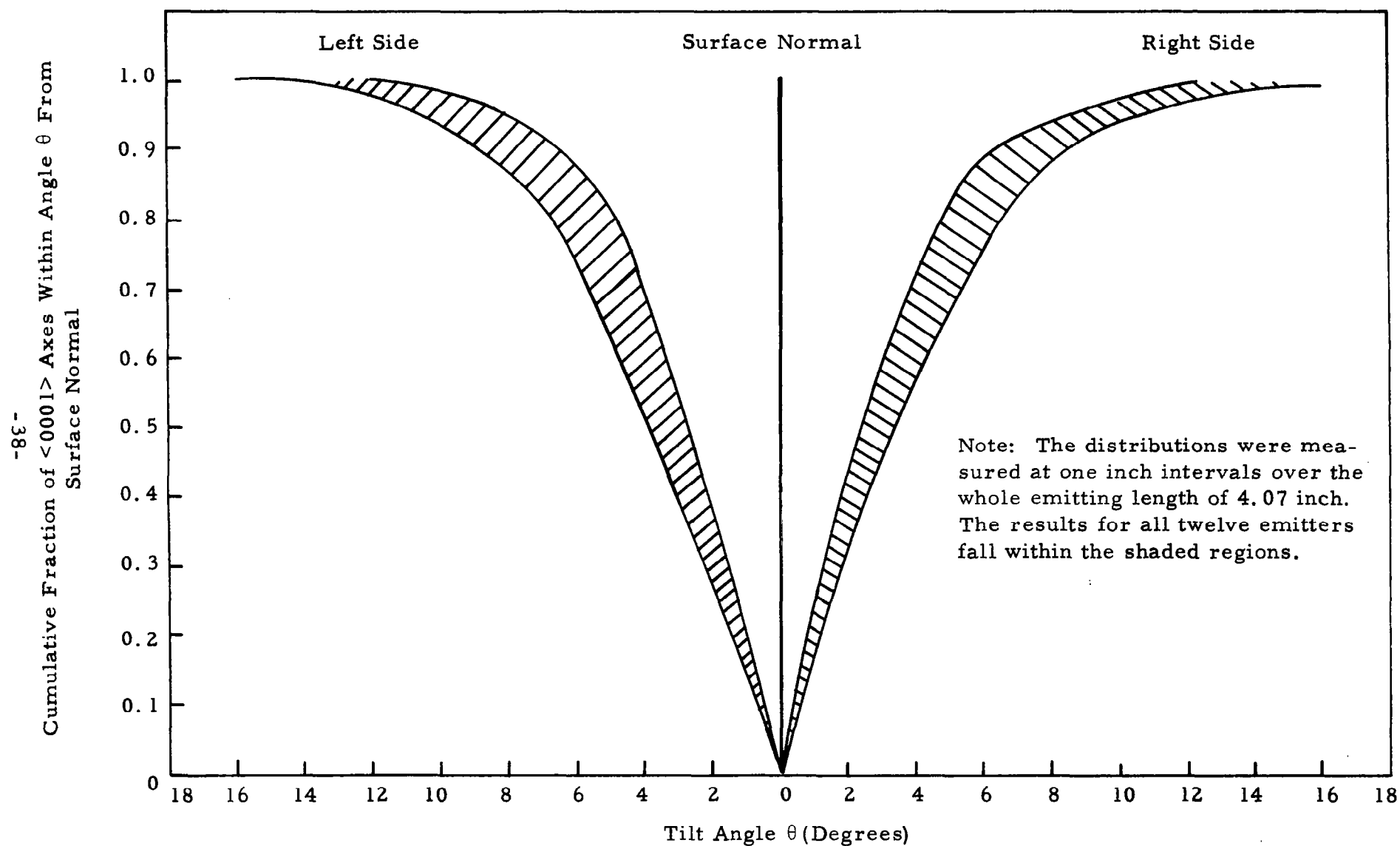


Fig. 14. Distributions of the $\langle 110 \rangle$ axes in cylindrical duplex tungsten emitters, numbers 1 through 12

preferred crystal orientation and vacuum work function of chloride-fluoride duplex tungsten emitters, it is concluded that these emitters should possess vacuum work functions of 4.9 eV or better.

REFERENCES

1. Wichner, Ronald and Thomas H. Pigford, "Work Functions of Monocrystalline and Polycrystalline Rhenium," Conference Record of 1966 Thermionic Conversion Specialist Conference, p. 405.
2. Pigford, Thomas H. and Byron E. Thinger, "Performance Characteristics of a 0001 Rhenium Thermionic Converter," Conference Record of 1969 Thermionic Conversion Specialist Conference, p. 34.
3. Glaski, Fred A., "The Formation of (0001) Oriented Rhenium Surfaces by Chemical Vapor Deposition," Conference Record of 1970 Thermionic Conversion Specialist Conference, p. 128.
4. Hudson, R. G. and L. Yang, "Diffusion and Electron Emission Properties of Duplex Refractory Metal Thermionic Emitters," Metallurgical Society Conferences, Volume 41, Refractory Metals and Alloys IV, Research and Development, Volume II, p. 1253.
5. Summary Report for the Period June 1, 1968 through January 31, 1971, Contract NAS 3-11822, NASA CR-120839, Gulf-GA-A11049.

DISTRIBUTION LIST

1. National Aeronautics and Space Administration
400 Maryland, S. W.
Washington, D. C. 20546
Attention: James J. Lynch, Code NS-1 (1)
Carl Johnson, Code NS-1 (1)
2. National Aeronautics and Space Administration
Lewis Research Center
21000 Brookpark Road
Cleveland, Ohio 44135
Attention: Report Control, MS 5-5 (1)
Technology Utilization Office, MS 3-19 (1)
Library, MS 60-3 (1)
G. M. Ault, MS 3-13 (1)
Neal Saunders, MS 105-1 (1)
John W. R. Creagh, MS 49-2 (1)
Leonard W. Schopen, MS 500-206 (1)
Roland Breitwieser, MS 302-1 (1)
James Ward, MS 302-1 (1)
Armin F. Lietzke, MS 49-3 (1)
Vince Hlavin, MS 3-10 (1)
S. J. Kaufman, MS 49-2 (1)
P. L. Donoughe, MS 49-3 (2)
J. R. Smith, MS 49-3 (4)
3. National Aeronautics and Space Administration
Manned Spacecraft Center
Attention: Technical Information Program Division
Houston, Texas 77058
For: B. J. Bragg (1)
W. Eugene Rice (1)
4. National Aeronautics and Space Administration
Marshall Space Flight Center
Huntsville, Alabama 35812
Attention: Library
For: Robert Aden (1)

5. National Aeronautics and Space Administration
Scientific and Technical Information Facility
P. O. Box 33
College Park, Maryland 20740
Attention: NASA Representative (10 copies)
6. National Aeronautics and Space Administration
Ames Research Center
Moffett Field, California 94035
Attention: Library (1)
7. National Aeronautics and Space Administration
Goddard Space Flight Center
Greenbelt, Maryland 20771
Attention: Library (1)
Joseph Epstein (1)
8. National Aeronautics and Space Administration
Langley Research Center
Langley Field, Virginia 23365
Attention: Library (1)
9. Aerojet General Nucleonics
San Ramon, California 94583
Attention: Library (1)
10. Aerospace Corporation
P. O. Box 95085
Los Angeles, California 90045
Attention: Library (1)
11. Air Force Cambridge Research Laboratories
L. G. Hanscom Field
Bedford, Massachusetts 01731
Attention: CRZAP (1)
12. Air Force Weapons Laboratory
Kirtland Air Force Base
New Mexico 87117
Attention: Library (1)
13. Babcock and Wilcox Company
1201 Kemper Street
Lynchburg, Virginia 24501
Attention: Library (1)

14. Battelle Memorial Institute
505 King Avenue
Columbus, Ohio 43201
Attention: Don Kizer (1)
Don Keller (1)
15. The Boeing Company
P. O. Box 3707
Seattle, Washington 98101
Attention: Library (1)
16. Electro-Optical Systems, Inc.
300 North Halstead Street
Pasadena, California 91107
Attention: A. Jensen (1)
17. Fairchild-Hiller
Republic Aviation Division
Farmingdale, L. I., New York 11735
Attention: Alfred Schock (1)
18. General Electric Company
Research Laboratory
Schenectady, New York 12300
Attention: Volney C. Wilson (1)
19. General Electric Company
Missile and Space Division
P. O. Box 8555
Philadelphia, Pennsylvania 19101
Attention: ANSE (1)
20. General Electric Company
Knolls Atomic Power Laboratory
Schenectady, New York 12300
Attention: R. Ehrlich (1)
21. Institute for Defense Analysis
400 Army Navy Drive
Arlington, Virginia 48092
Attention: R. C. Hamilton (1)

22. McDonnell Douglas Corporation
Missile and Space Engineering
Nuclear Research (A2-260)
3000 Ocean Park Boulevard
Santa Monica, California 90405
Attention: Library (1)
23. Jet Propulsion Laboratory
California Institute of Technology
4800 Oak Grove Drive
Pasadena, California 91103
Attention: Peter Rouklove (1)
J. Mondt (1)
V. Truscello (1)
24. Lockheed Missile and Space Division
Lockheed Aircraft Corporation
Sunnyvale, California 94086
Attention: H. H. Greenfield (1)
25. Los Alamos Scientific Laboratory
P. O. Box 1663
Los Alamos, New Mexico 87544
Attention: W. A. Ranken (1)
26. Naval Ship Systems Command
Department of the Navy
Washington, D. C. 20360
Attention: E. P. Lewis, Code 08 (1)
27. North American Rockwell Corporation
Atomics International Division
P. O. Box 309
Canoga Park, California 91305
Attention: Robert C. Allen (1)
Charles E. Smith (1)
28. North American Rockwell Corporation
S&ID Division
12214 Lakewood Boulevard
Downey, California 90241
Attention: C. L. Gould (1)
29. Oak Ridge National Laboratory
Oak Ridge, Tennessee 37831
Attention: Library
For: A. C. Schaffhauser (1)

30. Office of Naval Research
Power Branch
Department of the Navy
Washington, D. C. 20325
Attention: Cmdr. Ollie J. Loper (1)
31. Radiation Effects Information Center
Battelle Memorial Institute
505 King Avenue
Columbus, Ohio 43201
Attention: R. E. Bowman (1)
32. Radio Corporation of America
David Sarnoff Research Center
Princeton, New Jersey 08640
Attention: Paul Rappaport (1)
33. The Rand Corporation
1700 Main Street
Santa Monica, California 90401
Attention: Ben Pinkel (1)
34. Space Systems Division (SSTRE)
AF Unit Post Office
Los Angeles, California 90045
Attention: Major W. Iller (1)
35. Thermo Electron Corporation
85 First Avenue
Waltham, Massachusetts 02154
Attention: George Hatsopoulous (1)
Robert Howard (1)
36. TRW Inc.
TRW Systems Group
One Space Park
Redondo Beach, California 90278
Attention: Library (1)
37. U. S. Army Erdl
Fort Monmouth, New Jersey 07703
Attention: Emil Kittl (1)
38. U. S. Atomic Energy Commission
Space Nuclear Systems Division, F309
Reactor Power Systems Branch
Washington, D. C. 20545
Attention: D. S. Beard (1)

39. U. S. Atomic Energy Commission
Technical Reports Library
Washington, D. C. 20545
Attention: J. M. O'Leary (3)
40. U. S. Atomic Energy Commission
Division of Technical Information Extension
P. O. Box 62
Oak Ridge, Tennessee 37831 (3)
41. Varian Associates
611 Hansen Way
Palo Alto, California 94308
Attention: Ira Weismann (1)
42. Westinghouse Electric Corporation
Astronuclear Laboratory
Attention: Documen Custodian
P. O. Box 10864
Pittsburgh, Pennsylvania 15236
For: Carrol Sinclair (1)